The Journal of Immunology

CD8+ T Cells Suppress Viral Replication in the Cornea but Contribute to VEGF-C–Induced Lymphatic Vessel Genesis

Christopher D. Conrady, Min Zheng, Donald U. Stone and Daniel J. J. Carr

J Immunol 2012; 189:425-432; Prepublished online 30 May 2012;
doi: 10.4049/jimmunol.1200063
http://www.jimmunol.org/content/189/1/425

The Journal of Immunology is published twice each month by
The American Association of Immunologists, Inc.,
1451 Rockville Pike, Suite 650, Rockville, MD 20852

Print ISSN: 0022-1767 Online ISSN: 1550-6606.

CD8$^+$ T Cells Suppress Viral Replication in the Cornea but Contribute to VEGF-C–Induced Lymphatic Vessel Genesis

Christopher D. Conrady,* Min Zheng,† Donald U. Stone,† and Daniel J. J. Carr*,†

HSV-1 is the leading cause of infectious corneal blindness in the industrialized world. CD4$^+$ T cells are thought to be the major leukocyte population mediating immunity to HSV-1 in the cornea as well as the likely source of immunopathology that reduces visual acuity. However, the role of CD8$^+$ T cells in immune surveillance of the cornea is unclear. Thus, we sought to evaluate the role of CD8$^+$ T cells in ocular immunity using transgenic mice in which >98% of CD8$^+$ T cells are specific for the immunodominant HSV-1 epitope (gBT-I.1). We found a significant reduction in virus, elevation in HSV-specific CD8$^+$ T cell influx, and more CD8$^+$ T cells expressing CXCR3 in the cornea of transgenic mice compared with those in the cornea of wild-type controls yet similar acute corneal pathology. However, by day 30 postinfection, wild-type mice had drastically more blood and lymphatic vessel projections into the cornea compared with gBT-I.1 mice, in which only lymphatic vessel growth in response to VEGF-C could be appreciated. Taken together, these results show that CD8$^+$ T cells are required to eliminate virus more efficiently from the cornea but play a minimal role in immunopathology as a source of VEGF-C. *The Journal of Immunology*, 2012, 189: 425–432.

Herpes simplex virus type 1 is a neurotropic, dsDNA virus proven to be a highly successful pathogen based on seroconversion of the adult population in excess of 60% (1). The virus is spread through a mucocutaneous route, where it first invades host epithelium eventually to gain access to sensory nerve fibers. HSV-1 is then transported in a retrograde fashion to the cell body that populates sensory ganglia such as the trigeminal ganglia where the virus persists in a latent state (2). The virus can then sporadically reactivate in response to stressors (e.g., environmental stressors including UV exposure, temperature changes, and intellectual challenge) sending infectious virions down the maxillary or mandibular branch of the trigeminal nerve by anterograde transport to produce a lesion or "cold sore" on or near the labium. In stark contrast to labial lesions, more atypical presentations include primary or recurrent infection (reactivation) that induces significant yet devastating pathology in the CNS (i.e., encephalitis) (3) and cornea.

In the cornea, a site innervated by the ophthalmic division of the trigeminal nerve, HSV-1 can periodically reactivate to induce recurrent inflammatory conditions (4) in the stroma or epithelium known as epithelial or stromal keratitis (herpetic stromal keratitis; HSK), respectively. In the stroma, the disease can progress to result in significant and permanent scarring and is the leading cause of infectious corneal blindness in the developed world (5). The cornea relies on transparency and proper shape to filter light to the lens and retina. Any alteration (i.e., inflammatory insults and scarring) to light passage in the eye can have drastic effects on visual acuity. Thus, understanding the immune response to HSV-1 in the cornea and the perpetual effects of these responses is critical in tailoring treatments to eradicate the virus while limiting permanent pathology that severely affects vision. Current experimental evidence suggests that a vast portion of the pathology during HSK episodes is likely orchestrated by infiltrating neutrophils (6, 7) and CD4$^+$ T cells (8, 9). Reports have even shown that CD4$^+$ T cells localize to areas of keratitis (10).

Conversely, the CD8$^+$ T cell-driven immune response is crucial in the containment of HSV-1 in tissues outside of the cornea (11, 12). Mice deficient in innate type I IFN signaling (type I IFN receptor A1 or CD118$^{-/-}$) are extremely susceptible to rapid HSV-1 dissemination; however, when HSV-specific CD8$^+$ T cells are adoptively transferred into CD118$^{-/-}$ mice, recipients show a significant reduction in the viral load of the brain stem and trigeminal ganglia (13). These results highlight the importance of CD8$^+$ T cells in immune surveillance of HSV-1 in neuronal tissue but fail to address whether CD8$^+$ T cells are necessary to control HSV-1 replication in the cornea.

Although several groups have attempted to describe the function of CD8$^+$ T cells in ocular immunity to HSV-1, they have failed to address a definitive role of CD8$^+$ T cells in clearing HSV-1 and/or inducing ocular pathology during the initial stages of infection. Models employing knockout mice for CD4$^+$ and CD8$^+$ T cell populations have been used to evaluate the specific roles of CD4$^+$ and CD8$^+$ T cells (9, 14–16). In terms of the role of CD8$^+$ T cells, two recent reports described the importance of a CD4$^+$ T cell influx regulating CD8$^+$ T cell entry into mucosal sites after infection (17) as well as an inherent role of CD4$^+$ T cells in priming of CD8$^+$ T cells to attain competent IFN-γ and TNF-α production in response to HSV-1 (18). Consequently, abolishing CD4$^+$ T cells could hinder CD8$^+$ T cell access to the infected cornea and diminish their effector function, clouding conclusions drawn from these studies. Relative to CD8$^+$ T cells in the presence of CD4$^+$ T lymphocytes, only two reports have evaluated viral replication during acute infection. One report measured viral shedding into the tear film and found no difference in mice with or without CD8$^+$ T cells (19). However, another group reported a rise

*Department of Microbiology and Immunology, University of Oklahoma Health Sciences Center, Oklahoma City, OK 73104; and †Department of Ophthalmology, University of Oklahoma Health Sciences Center, Oklahoma City, OK 73104

Received for publication January 13, 2012. Accepted for publication April 30, 2012.

This work was supported in part by National Institutes of Health Grant EY021238 (to D.J.J.C.). Additional support includes an unrestricted grant from Research to Prevent Blindness (P20 RR017703) and a University of Oklahoma Health Sciences Center Presbyterian Health Foundation Presidential Professorship award (to D.J.J.C.).

Address correspondence and reprint requests to Dr. Daniel J.J. Carr, Department of Ophthalmology, DMEI #415, University of Oklahoma Health Sciences Center, 608 Stanton L. Young Boulevard, Oklahoma City, OK 73104. E-mail address: dan-carr@ouhsc.edu

Abbreviations used in this article: gB, glycoprotein B; HSK, herpetic stromal keratitis; MLN, mandibular lymph node; WT, wild-type.

in infectious virus in the periocular skin and tear film in the absence of CD8$^+$ T cells during acute infection (16). On the basis of the discrepancy in the literature on the role of CD8$^+$ T cells in viral surveillance within the cornea after infection, we initiated a study using mice in which >98% of CD8$^+$ T cells are HSV-1 specific (20). These mice were previously found to be useful in establishing the importance of HSV-specific CD8$^+$ T cells in limiting virus egress in a cutaneous model of infection (21).

Thus, we hypothesized that CD8$^+$ T cells were critical in inhibiting viral replication in the cornea in response to HSV-1 infection while contributing to immune-mediated pathology that others have attributed to CD4$^+$ T cells. However, in the current study we found that although CD8$^+$ T cells actively participate in containing HSV-1 replication, their presence in the cornea was not associated with more severe pathology (i.e., MMP-9 expression and slit lamp examination) despite their contribution to the production of VEGF-C and lymphangiogenesis.

Materials and Methods

Mice and virus

C57BL/6J wild-type (WT) mice were purchased from The Jackson Laboratory (Bar Harbor, ME). HSV glycoprotein B (gB)T-I.1 TCR transgenic mice (20) on a WT background were maintained in the Dean McGee Eye Institute's animal facility and were all genotyped to confirm the presence of the transgene. gBT-I.1 mice were back-crossed with CXCR3$^{-/-}$ mice (22) and genotyped to confirm transgene and knockout. Animal treatment was consistent with the National Institutes of Health *Guide for the Care and Use of Laboratory Animals*, and all procedures were approved by the University of Oklahoma Health Sciences Center and Dean A. McGee Eye Institute Institutional Animal and Care Use Committee. HSV-1 (strain McKrae) was propagated in green monkey kidney cells (Vero cells), titered, and stored at −80°C as previously described (13).

HSV-1 infection

Six- to ten-week-old male and female WT, gBT-I.1, and gB-CXCR3$^{-/-}$ sex-matched mice were anesthetized by an i.p. injection of xylazine (6.6 mg/kg) and ketamine (100 mg/kg). Their corneas were scarified using a 25-gauge 1½-in. needle and tear film blotted. HSV-1 McKrae (1000 PFU) was resuspended in 3 μl sterile 1× PBS and then topically inoculated onto the scarified corneas. HSV-1 viral titers in the cornea were determined 3 and 7 d postinfection by plaque assay as previously described (13).

Histochemistry

WT and gBT-I.1 mice were infected with HSV-1. Whole eyes were harvested, fixed in 4% paraformaldehyde for 24 h at 4°C, transferred to 70% ethanol, and embedded in paraffin. Five-micrometer sections were cut and mounted on slides. H&E staining was then performed as well as a one-step trichrome (Gomori's) stain. Uninfected WT and gBT-I.1 mice served as negative controls. Images were then captured using a Nikon Eclipse E800 Epifluorescent microscope (Nikon, Melville, NY) at ×40, ×100, and ×200 magnifications.

Slit lamp exam

The corneas of both WT and gBT-I.1 mice were examined 7 d postinfection for clinical pathology by a "masked" ophthalmologist using a Kowa portable slit lamp (Kowa Optimed, Torrance, CA). Corneal pathology was assessed using the following scoring key: 0 = no pathology; 1 = injected eye, no opacity; 2 = focal opacity; 3 = hazy opacity over entire cornea; 4 = dense opacity in central cornea with remainder hazy; 5 = same as no. 4 but with ulcer; and 6 = corneal perforation.

ELISAs

At the appointed time, infected gBT-I.1 and WT mice were euthanized and perfused with 1× PBS. Corneas were harvested and resuspended in 1× PBS with a protease mixture (Calbiochem, La Jolla, CA). After tissue homogenization, supernatants were clarified with a 10,000 × *g* spin for 1.5 min. Supernatants were then subjected to sandwich ELISAs (R&D Biosystems, Minneapolis, MN) and suspension arrays (Bio-Rad, Hercules, CA) to measure MMP-9, CXCL1, CCL2, CCL5, CXCL9, and CXCL10 levels 7 d postinfection as previously described (13).

Flow cytometry

Briefly, corneas, draining mandibular lymph nodes (MLNs), and blood (by retroorbital bleed) were harvested from WT and gBT-I.1 mice 0 or 7 d postinfection. The tissues were then processed by passing through a 40-μm filter to create single-cell suspensions that were subsequently labeled with anti-CD8, anti-CD4, anti-NK1.1, anti-CD3, anti-CXCR3, anti-CCR5, anti-CD45 (BD Biosciences, San Jose, CA), and/or tetramer (Baylor College of Medicine, Houston, TX) to identify specific leukocyte populations. The cell suspensions were washed in 1% BSA/PBS and fixed in 1% paraformaldehyde overnight. The samples were then analyzed by flow cytometry (Beckman Coulter, Brea, CA) with known amounts of Count-Bright beads (Invitrogen, Eugene, OR) as previously described to evaluate total cell numbers found in the respective tissue (13).

Intracellular staining

Single-cell suspensions were isolated as described above from the draining MLNs of WT and gBT-I.1 mice 7 d postinfection. One million cells were resuspended in 1.0 ml RPMI 1640 medium containing 10% FBS and added to 24-well culture plates. Cells were stimulated with 2 μg HSV-specific gB peptide (SSIEFARL) (Biomatik USA, Wilmington, DE) for 1 h at 37°C at which point 1 μl brefeldin A (BD Biosciences) was added. After an additional 3 h at 37°C, nonspecific Ab binding was inhibited with 2 μl Fc block (BD Biosciences) for 15 min at 4°C. Select extracellular receptors were then stained with PE–Cy5–conjugated CD45 and FITC-conjugated CD8 for 30 min at 4°C. The cells were permeabilized according to the manufacturer's protocol (BD Biosciences). After permeabilization, cells were stained with 4 μl PE-conjugated IFN-γ (BD Biosciences) at 4°C and twice washed. The single-cell suspensions were analyzed by flow cytometry as described above.

Confocal imaging

Corneas were harvested from both WT and gBT-I.1 mice at 0, 7, and 30 d postinfection. The corneas were fixed in 4% paraformaldehyde and washed in 1% PBS–Triton as previously described (23). The tissue was blocked with Fc block overnight at 4°C and then incubated with primary Ab against CD31 (Millipore) and Lyve 1 (Abcam) overnight at 4°C. After three washes with 1% PBS–Triton, secondary Abs were added (Jackson ImmunoResearch Laboratories) and incubated overnight at 4°C. After three more washes, corneas were incubated at 4°C with DAPI overnight. Corneas were then mounted and imaged as z-stack images using an epifluorescence/confocal laser-scanning microscope (IX81-FV500; Olympus) as previously described (23).

CD8$^+$ T cell depletion

gBT-I.1 transgenic mice were infected with 1000 PFU/eye HSV-1. After 30 min, gBT-I.1 mice were given a subconjunctival injection of either 40 μg anti-CD8a (Bio X cell, Lebanon, NH) or isotype Ab (rat IgG) resuspended in 10 μl 1× PBS. The mice were then treated again with 40 μg Ab at 2, 4, and 6 d postinfection. At 7 d postinfection, mice were euthanized and viral content assessed in the cornea by plaque assay as previously described, VEGF isoform expression by RT-PCR, or lymphatic growth by confocal microscopy. Depletion was confirmed by flow cytometric analysis of the cornea for CD8$^+$ T cell population as previously described.

VEGF-C neutralization

gBT-I.1 mice were infected as previously described. Three days postinfection and every other day thereafter, mice were given a 10-μl subconjunctival injection (10 μg total) of either human IgG or VEGFR3-Fc (R&D Systems). Lymphatic growth was then evaluated 7 d postinfection by confocal microscopy as described previously.

RT-PCR

mRNA was isolated from infected and uninfected gBT-I.1 and WT corneas as previously described (24). Briefly, corneas were harvested and homogenized. Total RNA was then isolated using TRIzol per the manufacturer's guidelines (Invitrogen). cDNA was synthesized using avian myeloblastosis reverse transcriptase and real-time PCR performed with an iCycler. Primer sequences have been previously described (25). To evaluate mRNA expression of trafficking leukocyte populations, MLN and spleen leukocytes were pooled from uninfected and infected mice (day 7 postinfection), and 1×10^7 cells were subjected to a CD8$^+$ isolation column (Miltenyi Biotec) to isolate CD8$^+$ cells from all others per the manufacturer's protocol. RT-PCR was then performed to identify sources of VEGF isoform expression. Flow cytometric analysis was performed to evaluate purity of populations.

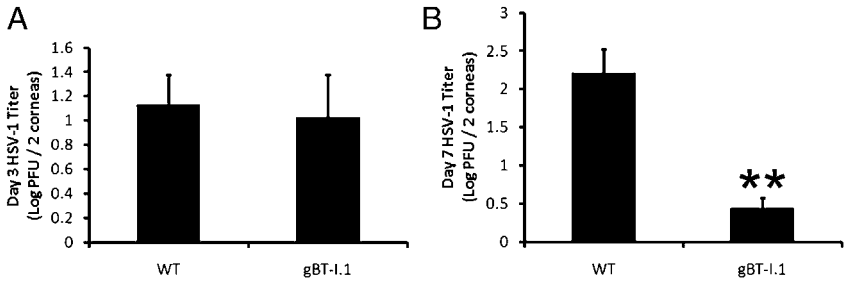

FIGURE 1. gBT-I.1 mice harbor significantly less virus by day 7 postinfection than that of WT controls. WT and gBT-I.1 mice were infected with 1000 PFU/eye HSV-1. At the indicated time postinfection, mice were euthanized and corneas harvested. Viral levels in the cornea were evaluated by plaque assay 3 d (**A**) and 7 d (**B**) postinfection. Results represent two to four independent experiments of two to three mice per group and are expressed as the mean log PFU/cornea ± SEM. $^{**}p < 0.01$ (comparing gBT-I.1 to WT mice).

Statistics

Statistical analysis was performed using the GBSTAT program (Dynamic Microsystems, Silver Spring, MD). A Student *t* test was used to determine significant ($p < 0.05$) differences between WT and gBT-I.1 groups.

Results

gBT-I.1 transgenic mice harbor less virus yet have comparable acute corneal pathology to WT animals after ocular HSV-1 infection

$CD4^+$ T cells have been assumed to be the major adaptive leukocyte population driving immune clearance and pathology in the cornea (14, 15). Thus, we sought to evaluate the role, if any, $CD8^+$ T cells have in viral surveillance after ocular HSV-1 infection using transgenic mice in which nearly all of the $CD8^+$ T cells recognize the immunodominant HSV-1 gB peptide epitope (20). To evaluate the role of $CD8^+$ T cells in containing HSV-1 replication, WT and gBT-I.1 mice were ocularly infected with 1000 PFU and sacrificed either 3 or 7 d postinfection. Whereas viral loads were similar 3 d postinfection (Fig. 1A), infectious virus levels in the cornea of WT mice were 10–100 times higher than those of gBT-I.1 mice as determined by plaque assay by 7 d postinfection (Fig. 1B). To next evaluate whether a decreased viral load corresponded with an increase in pathology during the acute infection, we performed H&E staining to identify infiltrating leukocytes and trichrome staining to visualize collagen fiber destruction/rearrangement. Samples viewed by two masked individuals found no appreciable pathologic differences in the cornea of gBT-I.1 mice and of WT counterparts 7 d postinfection (Fig. 2). Both gBT-I.1 and WT mice had similar presentation of leukocytes residing in the cornea proper (Fig. 2A, 2B) as well as varying degrees of collagen fiber disruption (Fig. 2E, 2F) in comparison with WT and gBT-I.1 uninfected controls, which had no measurable leukocyte infiltrate or corneal pathology (Fig. 2C, 2D, 2G, 2H). Clinical slit lamp examination and MMP-9 protein levels were consistent with histological specimens in that corneas of infected gBT-I.1 mice had only modestly higher clinical scores and similar levels of MMP-9 expression compared with WT corneas (Fig. 3A, 3B). Furthermore, infected WT and gBT-I.1 mice showed significantly elevated corneal MMP-9 levels compared with their uninfected counterparts (<0.02 ng/mg cornea). To examine ocular pathology further, confocal imaging was performed to evaluate lymphatic and blood vessel growth into the cornea proper. By day 7 postinfection, both WT and gBT-I.1 mice had lymphatic vessels (yellow arrows, $Lyve1^{hi}$, $CD31^{lo}$, Fig. 3D) infiltrating the cornea, but only WT mice had appreciable blood vessel genesis ($CD31^+$, $Lyve1^-$) (Fig. 3C, 3D, and data not shown). The lack of blood vessel growth into gBT-I.1 cornea proper was only intensified by day 30 postinfection compared with WT controls (Fig. 3D, pink arrows). Taken together, gBT-I.1 mice had significantly less virus yet comparable levels of ocular pathology as WT controls during the acute phase of disease (0–7 d postinfection) suggesting viral loads were not a reliable predictor of HSK (day 30). These findings also further reiterated a likely immune-mediated role in corneal pathologic outcomes after HSV-1 infection.

HSV-specific $CD8^+$ T cells infiltrate HSV-1–infected corneas of gBT-I.1 mice far in excess of that found in WT controls

To identify contributing factors associated with viral surveillance in the cornea of gBT-I.1 mice after HSV-1 infection, leukocyte populations residing in the tissue were phenotypically identified. Whereas the percentage of total $CD8^+$ T cells was not different comparing WT to gBT-I.1 mice (Fig. 4B), there was a substantial difference in the absolute number of HSV-specific $CD8^+$ T cells in the cornea proper with significantly more found in that of gBT-I.1 mice (Fig. 4A, 4C). No other significant differences were found in leukocyte populations [i.e., NK cell (data not shown), $CD4^+$ T cell

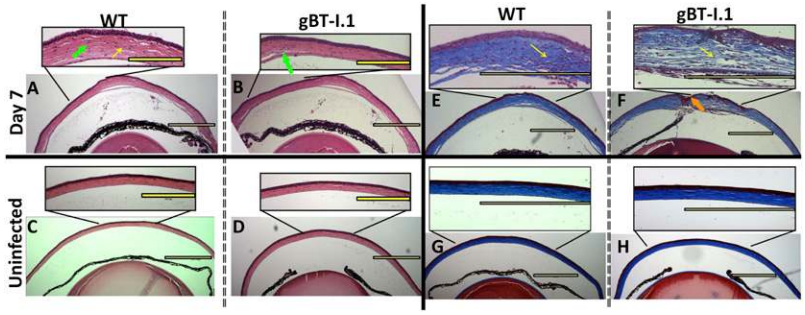

FIGURE 2. Histological assessment of corneas from HSV-1–infected gBT-I.1 transgenic and WT mice. WT and gBT-I.1 mice were infected with 1000 PFU/eye HSV-1. Seven days postinfection, corneas were harvested, fixed, sectioned, and stained with H&E to identify generalized leukocyte infiltration (**A**–**D**) or stained with Gomori's trichrome to evaluate collagen fiber disruption (**E**–**H**). WT mice (A) show leukocytes residing in the cornea proper similar to gBT-I.1 mice (B) and collagen fiber disruption as highlighted by the yellow arrow of the *inset* (A, E, and F). The orange arrow in (F) emphasizes sporadic ulcerations more typical of gBT-I.1 mice compared with WT animals. (C, D, G, and H) Representative images of uninfected controls. All depicted images are representative of three to four independent experiments of two to three eyes per group. Images are at ×40, ×100, or ×400 magnification. Yellow scale bars, 300 μm.

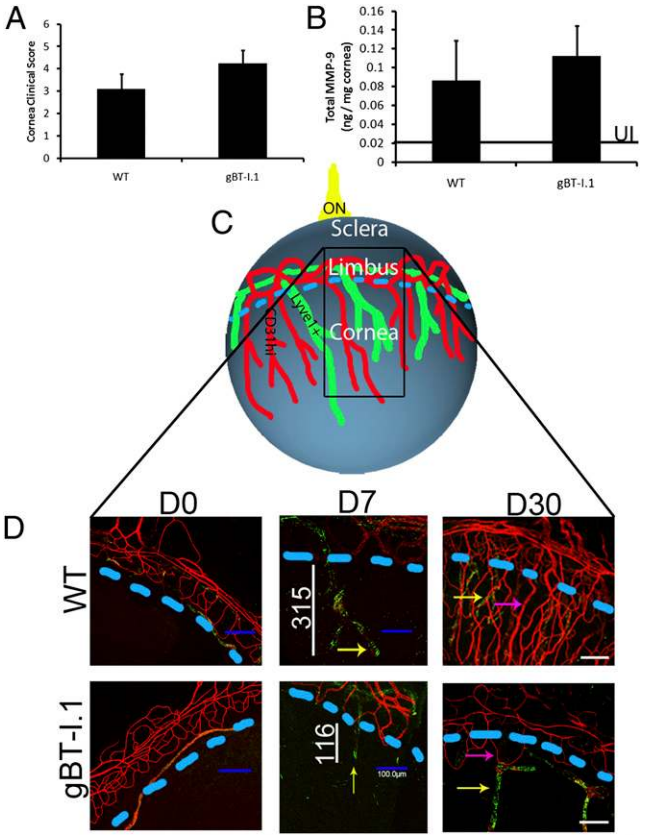

FIGURE 3. Ocular pathology in WT and gBT-I.1 mouse corneas. WT and gBT-I.1 mice were infected with 1000 PFU/eye HSV-1 McKrae. (**A**) At 7 d postinfection, clinical pathology was assessed and scored by a masked observer (clinical ophthalmologist) using a slit lamp examination, and no significant differences were identified. (**B**) MMP-9 expression was evaluated by ELISA and was similar in gBT-I.1 and WT mice after infection. Data are represented as the mean ± SEM. Values represent two independent experiments of two to three mice per group. Black line, MMP-9 expression in uninfected controls. (**C**) An overview of the cornea after HSV infection. Blue line, edge of cornea (limbus region); black box, area imaged; ON, optic nerve. (**D**) Corneas were then assessed for lymphatic (FITC, green, Lyve1^{hi}, CD31^{low}) and blood vessel (DyLight 549, red, CD31^{hi}) growth into the cornea proper at 0, 7, and 30 d postinfection. Pink arrows, blood vessel growth; yellow arrows, lymphatic vessel growth; white lines, length of lymphatic vessel; blue dashed lines, edge of cornea (limbus region).

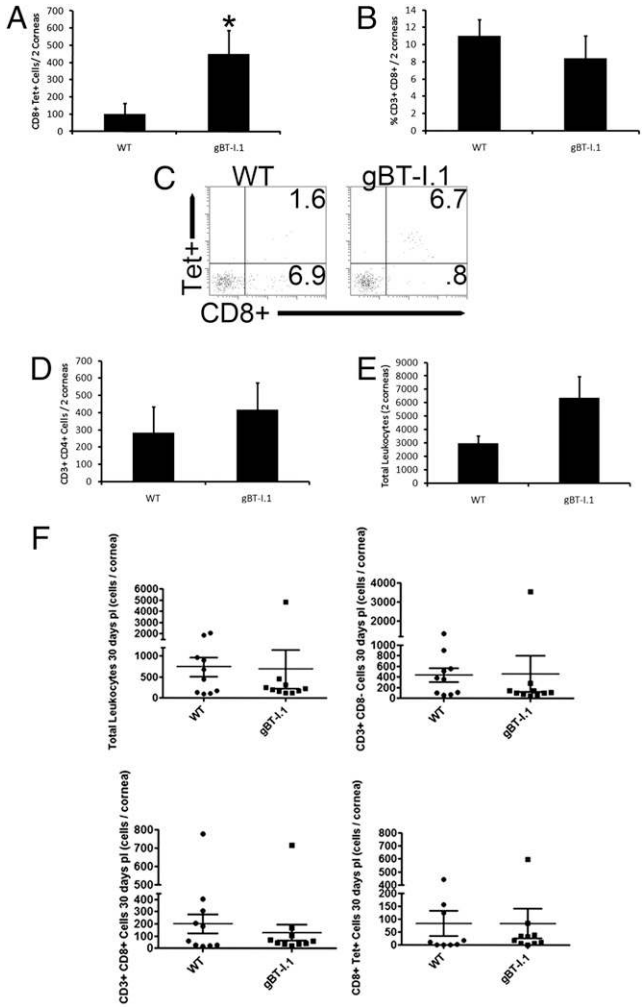

FIGURE 4. gBT-I.1 mice have a dramatic influx of HSV-specific CD8$^+$ T cells into the cornea not seen in WT. WT and gBT-I.1 mice were infected with 1000 PFU/eye HSV-1. At 7 or 30 d postinfection, the animals were exsanguinated, and the corneas were harvested, processed, and phenotypically characterized for leukocyte content by flow cytometry. (**A**) The HSV-specific CD8$^+$ T cell number 7 d postinfection. (**B**) Total CD8$^+$ T cells in the cornea 7 d postinfection. (**C**) A representative histogram for the corresponding results reported in (A). CD4$^+$ T cells and total leukocyte (CD45^{hi}) numbers 7 d postinfection are expressed in (**D**) and (**E**), respectively. Results from 30 d postinfection for CD8$^+$ T cells, CD3$^+$ CD8$^-$ cells, HSV-specific CD8$^+$ T cells, and total leukocytes are quantified in (**F**). Results in (A, B, D–F) are expressed as the mean ± SEM from two to three independent experiments of two to three mice per group. *$p < 0.05$ (comparing WT to gBT-I.1).

(Fig. 4D), and total leukocyte influx (Fig. 4E)] within the infected cornea comparing the two groups. Furthermore, this difference in HSV-specific CD8$^+$ T cells was not appreciated 3 d postinfection due to a lack of CD8$^+$ T cell infiltration (data not shown) and equilibrated by day 30 postinfection (Fig. 4F).

To determine if the results found in the cornea were reflective of that residing in the draining lymph nodes (MLNs) to explain the discrepancy in trafficking, select leukocyte populations including NK cells, CD4$^+$ and CD8$^+$ T cells, HSV-specific CD8$^+$ T cells, and total leukocytes were assessed 7 d postinfection. HSV-1–infected gBT-I.1 mice exhibited gross deficiencies in NK cells (Fig. 5B) and CD4$^+$ T cells (Fig. 5C), yet had significantly more HSV-specific and total CD8$^+$ T cells in the MLN compared with WT mice (Fig. 5A, 5D). Furthermore, there was a marked increase in the activation of CD8$^+$ T effector cells in response to HSV Ag in the total CD8$^+$ T cell population from the MLN of HSV-1–infected gBT-I.1 mice as determined by IFN-γ expression (Fig. 5E) and less regulatory T cells per effector CD8$^+$ T cell (Fig. 5F). We interpret these results to suggest gBT-I.1 mice are more adept at containing HSV-1 in the cornea due to increased HSV-specific CD8$^+$ T cell numbers that are capable of responding to viral Ag.

Enhanced recruitment of CD8$^+$ T cells into the cornea of gBT-I.1 mice is associated with an increased expression of chemokine receptor CXCR3

To explain the increased CD8$^+$ T cell trafficking into the cornea of gBT-I.1 mice, chemokine levels of known effector T cell chemoattractants (26–28) as well as inflammatory chemokines were evaluated. T cell chemoattractants including CCL5 and CXCL10 levels were significantly lower in the cornea of gBT-I.1 mice in comparison with those in the cornea of WT controls (Fig. 6A). Although CXCL9 was lower as well, the difference was not statistically different (Fig. 6A). Likewise, CCL2 but not CXCL1 was elevated in cornea tissue from HSV-1–infected WT mice in

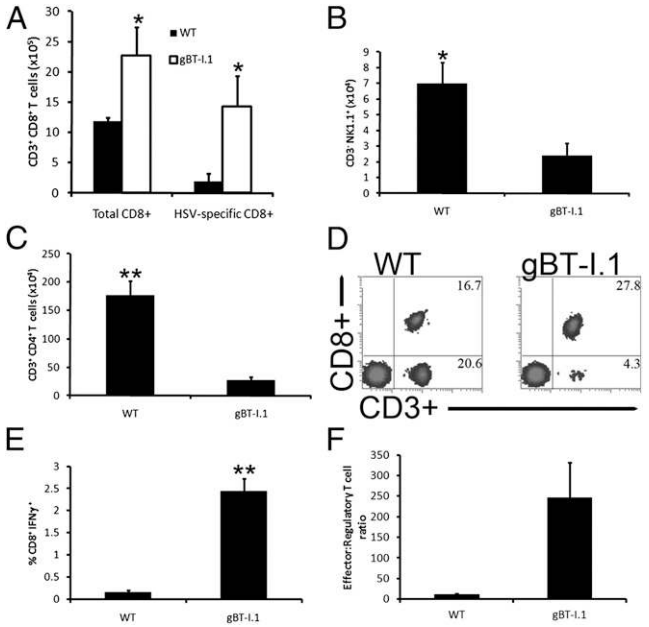

FIGURE 5. gBT-I.1 mouse draining MLNs possess significantly more total and HSV-specific CD8$^+$ T cells in comparison with WT. WT and gBT-I.1 mice were infected with 1000 PFU/eye HSV-1. At 7 d postinfection, leukocytes were isolated from the draining MLNs, and phenotypic profiles were analyzed by flow cytometry. gBT-I.1 mouse MLNs contained substantially more HSV-specific and total CD8$^+$ T cells than WT mice (**A**). Conversely, WT mice possessed significantly more CD3$^-$ NK1.1$^+$ (NK cells) and CD3$^+$ CD4$^+$ T cells in the MLN in comparison with gBT-I.1 mice (**B** and **C**). Representative histograms of flow analysis of CD3$^+$ CD8$^+$ T cells in the MLN is shown in (**D**). gBT-I.1 CD8$^+$ leukocytes were inherently more responsive to HSV-1 than WT cells as indicated by intracellular staining of IFN-γ in (**E**). Furthermore, gBT-I.1 mice had a higher effector to regulatory T cell (CD4$^+$ Foxp3$^+$) ratio than WT controls (**F**). Results summarize two to three experiments of two to three mice per group and are depicted as the mean leukocyte population ± SEM. $*p < 0.05$, $**p < 0.01$ (comparing gBT-I.1 and WT groups).

comparison with gBT-I.1 transgenic mice (Fig. 6B). Based on these results, chemokine expression parallels Ag load within the cornea of infected mice and does not alone explain the unique recruitment pattern found in the cornea of gBT-I.1 mice. As a result, chemokine receptor expression for the T cell chemoattractants CCL5, CXCL9, and CXCL10 was evaluated on the circulating CD8$^+$ T cell population after HSV-1 infection. The results show a significantly higher proportion of circulating CD8$^+$ T cells from gBT-I.1 mice express CXCR3 but not CCR5 in comparison with that found in WT mice and uninfected controls (Fig. 6C). To highlight further the importance of CXCR3, gBT.I-1 mice were back-crossed with CXCR3-deficient mice (gBT-I.1–CXCR3$^{-/-}$) and infected with HSV-1. gBT-I.1–CXCR3$^{-/-}$ mice had elevated HSV-1 titers in the cornea 7 d postinfection in comparison with gBT-I.1 controls, which was consistent among all three experiments (Fig. 6D). Collectively, these results emphasize the importance of CXCR3 expression on circulating CD8$^+$ T cells in immune surveillance in the cornea.

CD8$^+$ T cells contribute to immune surveillance and lymphatic growth after HSV-1 infection

To substantiate the contribution of CD8$^+$ T cells in gBT-I.1 mouse resistance to HSV-1 infection, CD8$^+$ T cells were depleted (Fig. 7A, 7C). In comparison with isotype control-treated mice, CD8$^+$ T cell-depleted gBT-I.1 mice possessed significantly more infectious virus in the cornea 7 d postinfection (Fig. 7B). These results substantiate the role of infiltrating CD8$^+$ T cells in immune surveillance of the cornea after ocular HSV-1 infection. To determine if the net loss of virus was correlative with a common pathologic condition of herpetic keratitis, angiogenesis was evaluated 7 d postinfection in isotype and CD8$^+$ T cell-depleted corneas (Fig. 7A, 7B). In gBT-I.1 mice depleted of CD8$^+$ T cells, lymphatic length was severely shortened (Fig. 7D), thus suggesting a role of CD8$^+$ T cells in lymphatic growth. From previous work in our laboratory, acute lymphatic growth was driven in response to VEGF-A production by infected epithelial cells during the first few days postinfection (25, 29). Thus, to identify the discrepancy in lymphatic and blood vessel genesis seen in WT and gBT-I.1 mice after infection (Fig. 3C), mRNA expression was evaluated for VEGF isoforms A, C, and D, which are known angiogenic factors (30). By day 5 postinfection, a significant elevation in VEGF-C could be appreciated in gBT-I.1 corneas compared with WT controls (Fig. 8B). Conversely, by day 30 postinfection, cor-

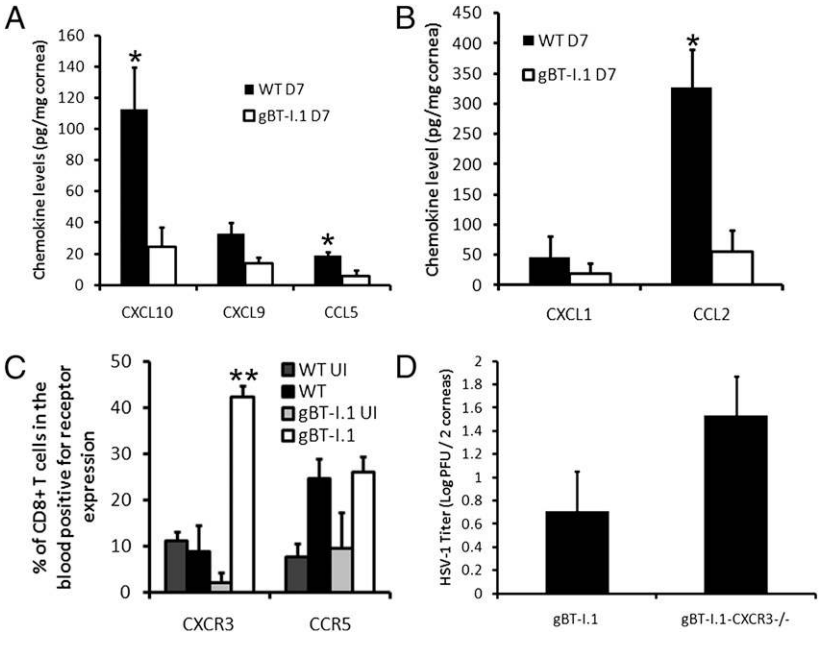

FIGURE 6. CXCR3 expression is elevated on circulating CD8$^+$ T cells. WT, gBT-I.1, and gB-CXCR3$^{-/-}$ mice (n = 4 to 6 mice/group) were infected with 1000 PFU/eye HSV-1. At 0 and 7 d postinfection, corneas were harvested and assayed for chemokine content by ELISA/suspension arrays. (**A**) WT mouse corneas possessed significantly more CCL5 and CXCL10 compared with gBT-I.1 mouse corneas. (**B**) WT mouse corneas expressed elevated levels of CCL2 but not CXCL1 in comparison with gBT-I.1 mouse corneas. (**C**) CXCR3 but not CCR5 expression is increased on CD8$^+$ T cells obtained from blood samples of gBT-I.1 mice in comparison with infected WT mice. (**D**) gB-CXCR3$^{-/-}$ harbored elevated levels of HSV-1 compared with gBT-I.1 mice as evaluated by plaque assay 7 d postinfection. Bars represent the mean ± SEM of two to three independent experiments. $*p < 0.05$, $**p < 0.01$ (comparing WT to gBT-I.1).

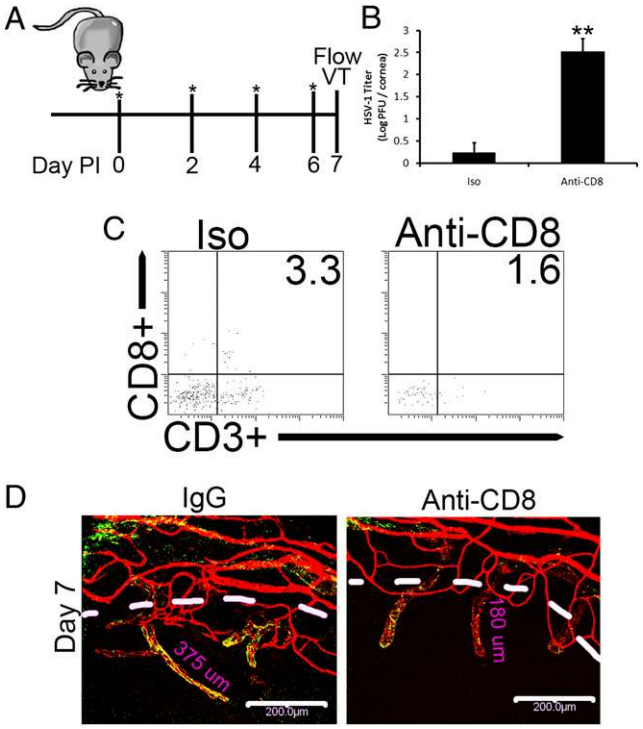

FIGURE 7. gBT-I.1 mice depleted of CD8$^+$ T cells have significantly higher viral titers in the cornea than isotype-treated gBT-I.1 mice yet shorter lymphatic vessels. gBT-I.1 mice were treated with anti-CD8a or isotype Ab the day of infection and every other day thereafter as depicted as asterisks in (**A**). At 7 d postinfection, corneas were harvested, and plaque assay was performed to evaluate infectious virion content (**B**) and flow cytometric analysis of the cornea (**C**) was performed to confirm CD8$^+$ T cell depletion. Representative histograms after treatment and infection can be seen in (**C**). Values are represented as the mean ± SEM of two independent experiments of two to three mice/group. (**D**) To investigate the role of CD8$^+$ T cells in angiogenesis, CD8$^+$ T cells were depleted and confocal imaging performed to evaluate lymphatic (FITC, green, Lyve1^{hi}, CD31^{lo}) and blood vessel growth (DyLight 549, red, CD31^{hi}). Images are representative of two experiments of two to four corneas per group. White scale bars, 200 µm; dashed white lines, border of cornea proper. $^{**}p < 0.01$.

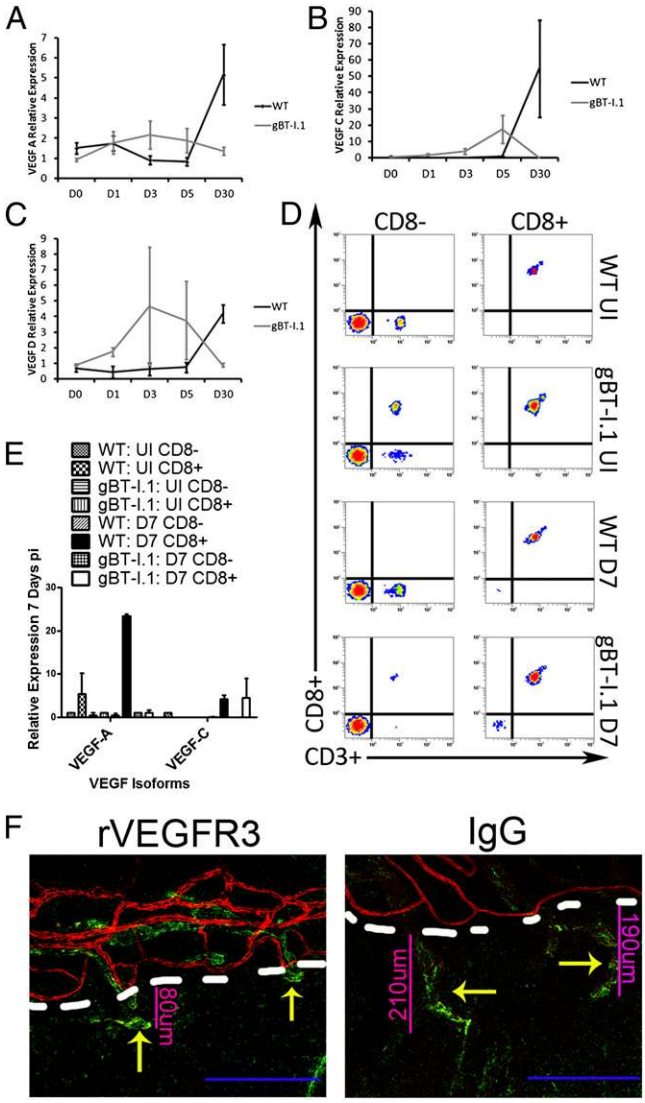

FIGURE 8. CD8$^+$ T cells secrete VEGF-C to induce lymphatic growth into the cornea. To evaluate the role of CD8$^+$ T cells in lymphangiogenesis, mRNA transcript expression for VEGF-A (**A**), VEGF-C (**B**), and VEGF-D (**C**) was evaluated 0, 1, 3, 5, or 30 d postinfection in WT and gBT-I.1 corneas. To then confirm that CD8$^+$ T cells were the major source of VEGF-C, CD8$^+$ and CD8$^-$ cell populations were isolated from the draining MLN and spleen and evaluated for VEGF expression (**E**), and purity was evaluated by flow cytometry (**D**). (**F**) To substantiate the role of VEGF-C in lymphatic growth, chimeric VEGFR3 or control IgG was ocularly administered to gBT-I.1 mice after infection and lymphatic (FITC, green, Lyve1^{hi}) and blood vessel (DyLight 549, red, CD31^{hi}) growth evaluated by confocal microscopy. Dashed white lines, border of cornea proper with limbus; yellow arrows, lymphatic vessels; pink lines, length of lymphatic vessel into the cornea proper.

neas of WT mice had significantly higher levels of all three isoforms tested than those of gBT-I.1 corneas (Fig. 8A–C). Previous work has shown that activated T cell lines can be a source of VEGF (31). To identify the role of CD8$^+$ T cells, if any, in lymphatic growth seen in gBT-I.1 mice, mRNA transcripts were evaluated from isolated infected and uninfected WT and gBT-I.1 draining MLNs and spleen (Fig. 8D). In both WT and gBT-I.1 mice, CD8$^+$ T cells were the major source of VEGF-C expression after infection (Fig. 8E). Notably, WT CD8$^+$ T cells were also a source of VEGF-A in an infected and uninfected setting (Fig. 8E). To substantiate the role of VEGF-C in lymphatic growth of gBT-I.1 corneas, VEGF-C neutralization was performed and resulted in a severe blunting of lymphatic growth by day 7 postinfection confirming VEGF-C–dependent lymphatic growth (Fig. 8F).

Discussion

In the current study, an increased influx of CD8$^+$ T cells into the cornea of gBT-I.1 mice after HSV-1 infection was associated with similar acute gross visual pathology with similar NK and CD4$^+$ T cell infiltration profiles and lower viral titers compared with WT controls. In patients suffering from HSK, HSV-specific CD8$^+$ T cells are found in relative abundance suggesting a role of CD8$^+$ T cells in inducing ocular pathology (32). In fact, mice deficient in CD4$^+$ T cell populations can still develop HSK (33), and the accumulation of activated CD4$^+$ T cells is not sufficient to cause the development of HSK further implicating a non-CD4$^+$ T cell population (34). From the results of the current study, CD8$^+$ T cells are not a major contributor to ocular pathology likely due to their ability to clear virus efficiently, thus reducing HSV-driven, VEGF-A–dependent lymphatic growth (25, 29). This is further supported in that a loss or depletion of CD8$^+$ T cells actually leads to enhanced neovascularization, opacity, and scarring (16, 19). However, the few unwarranted effects of these cells within the cornea likely results from the secretion of VEGF isoforms to initiate endothelial migration and proliferation (30). Although the

secretion of VEGF from T cells has been shown to induce a Th1 response required to inhibit HSV-1 spread and is likely important in tissues such as the lymph node (13, 31, 35), expression of VEGF in the cornea, more specifically VEGF-C, from $CD8^+$ T cells leads to detrimental lymphatic invasion of the avascular cornea. Lymphangiogenesis has severe visual consequences and is thus a tightly regulated phenomenon as evident by constitutive expression of soluble VEGFR-1 (36). Our laboratory had previously reported the importance of VEGF-A in lymphatic growth after HSV-1 infection (25). In the current study, VEGF-A is modestly increased in both WT and gBT-I.1 corneas within the first 24 h postinfection. The lower levels of HSV-driven VEGF-A could be due in part to the lower initial viral inoculum (29). We hypothesize that once VEGF-A has initiated lymphatic growth after HSV infection, VEGF-C then contributes to the vessel lengthening as evidenced by the shorter lymphatic vessels after VEGF-C neutralization compared with IgG controls.

Evidence clarifying the role of immune recognition and clearance of an HSV-1 infection of the cornea is a significant concern to the medical community. With recurrent bouts of herpetic keratitis, the incidence of corneal graft survival after transplantation is severely diminished [>90% (37) to <50% (38)], as well as increase of the frequency of corneal blindness due to infectious cause (1). Thus, a more complete understanding of immune-mediated events after HSV-1 infection could help alleviate the effect the immune response to HSV-1 has on corneal pathology while retaining the host's ability to control the pathogen. Broad-based therapies for HSK such as steroid-based eye drops used to suppress immune responses in the cornea leave the patient modestly immunocompromised (39). This treatment regimen could be supplanted with more specific inhibitors already clinically available for toxic molecules released by activated leukocytes including MMPs, TNF-α, and IFN-γ, all while retaining the host's ability to contain and eventually subdue the infection. Furthermore, addition of neutralization of VEGF isoforms with mAbs would result in less neovascularization (40) likely resulting in an additive reduction in long-term ocular pathology. Additionally, it is predicted that potential vaccines to inhibit HSV infections altogether would require a strong $CD8^+$ T cell activation component to abolish viral-driven VEGF-A production and thus lymphatic growth in the cornea (25, 29). Altogether, a vaccine toward HSV-1 and neutralizing Abs to VEGF would likely drastically attenuate ocular pathology.

Although the increased number of HSV-specific $CD8^+$ T cells in the cornea after infection is not associated with enhanced ocular pathology by clinical examination, the role of HSV-specific $CD8^+$ T cells in viral surveillance and clearance in the cornea should not be underestimated. We had previously described the importance of $CD8^+$ T cells in the CNS after HSV-1 infection (13) and hypothesized these cells were also required in the cornea to contain the virus. In the cornea of gBT-I.1 mice, the increased influx of HSV-specific $CD8^+$ T cells inversely correlated with viral titers 7 d postinfection despite no other identifiable leukocyte phenotypic difference between gBT-I.1 and WT mice. Moreover, neutralizing $CD8^+$ T cells enhanced gBT-I.1 mouse susceptibility to HSV-1 as seen by an increase in viral titer of $CD8^+$ T cell-depleted gBT-I.1 mice. Overall, the results point to a clear role for $CD8^+$ T cells as a contributing cell population in viral surveillance of the cornea.

The unique recruitment of $CD8^+$ T cells in gBT-I.1 mice could not be explained by chemokine production because of deficiencies in T cell chemoattractants CXCL9, CXCL10, and CCL5 production (41–43) compared with that in WT mice. Thus, circulating gBT-I.1 HSV-specific $CD8^+$ T cells were evaluated for CCR5 and CXCR3 expression. Even though the proportion of $CD8^+$ T cells expressing CXCR3 was significantly higher in gBT-I.1 than WT mice, this may not explain the story in its entirety. Although the importance of CXCR3 in regulating $CD8^+$ T cell trafficking is well described (27, 44), the role of chemokines and their receptors has expanded beyond strict immune trafficking to include functions of activation and immune suppression. CXCR3 has been shown to contribute to $CD8^+$ T cell activation in response to HSV-2 (45) and may initiate similar events in the cornea. Although we did not explore the exact deficiency, we speculate that gBT-I.1–$CXCR3^{-/-}$ mice harbored more virus in the cornea than did gBT-I.1 mice due to a loss of $CD8^+$ T cell trafficking and activation. We surmised that as a higher percentage of circulating $CD8^+$ T cells from gBT-I.1 mice expressed CXCR3 than the percentage of circulating $CD8^+$ T cells from WT mice that expressed CXCR3, the trafficking disparities and potentially increased activity/IFN-γ production of gBT-I.1 leukocytes is, in part, due to this phenomenon. This is supported by previous work in which $CXCR3^{-/-}$ -deficient mice have significantly higher viral titers than WT controls 7 d postinfection in the cornea proper (46). However, another group did not report similar findings (47) indicating the role of CXCR3 in the recruitment of lymphocytes and containment of virus in the cornea remains controversial.

Collectively, the results firmly establish a role for HSV-specific $CD8^+$ T cells in viral containment in the cornea, a role long attributed to $CD4^+$ T cells. Furthermore, the levels of HSV-1 do not correlate with severity of ocular pathology. Thus, the $CD8^+$ T cell immune response to HSV-1 in the cornea contains the virus but does result in a reduction of pathologic outcomes (hemangiogenesis), reiterating the major role of immune-mediated destruction of the cornea after infection. However, $CD8^+$ T cell expression of VEGF isoforms results in lymphatic growth into the cornea proper suggesting some role of $CD8^+$ T cells in lymphangiogenesis.

Acknowledgments

We thank Sara Moore for technical support and Dr. Carbone for the gBT-I.1 transgenic mice. We also thank Linda Boone and Louisa Williams for histology expertise and Fatemeh Shariati (all members of the Dean McGee Eye Institute CORE laboratory) for genotyping the gBT-I.1 and gBT-I.1–$CXCR3^{-/-}$ transgenic mice.

Disclosures

The authors have no financial conflicts of interest.

References

1. Xu, F., M. R. Sternberg, B. J. Kottiri, G. M. McQuillan, F. K. Lee, A. J. Nahmias, S. M. Berman, and L. E. Markowitz. 2006. Trends in herpes simplex virus type 1 and type 2 seroprevalence in the United States. *JAMA* 296: 964–973.
2. Khanna, K. M., A. J. Lepisto, and R. L. Hendricks. 2004. Immunity to latent viral infection: many skirmishes but few fatalities. *Trends Immunol.* 25: 230–234.
3. Conrady, C. D., D. A. Drevets, and D. J. Carr. 2010. Herpes simplex type I (HSV-1) infection of the nervous system: is an immune response a good thing? *J. Neuroimmunol.* 220: 1–9.
4. Carr, D. J., P. Härle, and B. M. Gebhardt. 2001. The immune response to ocular herpes simplex virus type 1 infection. *Exp. Biol. Med. (Maywood)* 226: 353–366.
5. Liesegang, T. J. 1989. Epidemiology of ocular herpes simplex. Natural history in Rochester, Minn, 1950 through 1982. *Arch. Ophthalmol.* 107: 1160–1165.
6. Yan, X. T., T. M. Tumpey, S. L. Kunkel, J. E. Oakes, and R. N. Lausch. 1998. Role of MIP-2 in neutrophil migration and tissue injury in the herpes simplex virus-1-infected cornea. *Invest. Ophthalmol. Vis. Sci.* 39: 1854–1862.
7. Duan, R., L. Remeijer, J. M. van Dun, A. D. Osterhaus, and G. M. Verjans. 2007. Granulocyte macrophage colony-stimulating factor expression in human herpetic stromal keratitis: implications for the role of neutrophils in HSK. *Invest. Ophthalmol. Vis. Sci.* 48: 277–284.
8. Doymaz, M. Z., and B. T. Rouse. 1992. Herpetic stromal keratitis: an immunopathologic disease mediated by CD4+ T lymphocytes. *Invest. Ophthalmol. Vis. Sci.* 33: 2165–2173.
9. Banerjee, K., P. S. Biswas, U. Kumaraguru, S. P. Schoenberger, and B. T. Rouse. 2004. Protective and pathological roles of virus-specific and bystander CD8+ T cells in herpetic stromal keratitis. *J. Immunol.* 173: 7575–7583.

10. Koelle, D. M., S. N. Reymond, H. Chen, W. W. Kwok, C. McClurkan, T. Gyaltsong, E. W. Petersdorf, W. Rotkis, A. R. Talley, and D. A. Harrison. 2000. Tegument-specific, virus-reactive CD4 T cells localize to the cornea in herpes simplex virus interstitial keratitis in humans. *J. Virol.* 74: 10930–10938.
11. Bonina, L., A. A. Nash, A. Arena, K. N. Leung, and P. Wildy. 1984. T cell-macrophage interaction in arginase-mediated resistance to herpes simplex virus. *Virus Res.* 1: 501–505.
12. Knickelbein, J. E., K. M. Khanna, M. B. Yee, C. J. Baty, P. R. Kinchington, and R. L. Hendricks. 2008. Noncytotoxic lytic granule-mediated CD8+ T cell inhibition of HSV-1 reactivation from neuronal latency. *Science* 322: 268–271.
13. Conrady, C. D., M. Thapa, T. Wuest, and D. J. Carr. 2009. Loss of mandibular lymph node integrity is associated with an increase in sensitivity to HSV-1 infection in CD118-deficient mice. *J. Immunol.* 182: 3678–3687.
14. Banerjee, K., P. S. Biswas, and B. T. Rouse. 2005. Elucidating the protective and pathologic T cell species in the virus-induced corneal immunoinflammatory condition herpetic stromal keratitis. *J. Leukoc. Biol.* 77: 24–32.
15. Hendricks, R. L., and T. M. Tumpey. 1991. Concurrent regeneration of T lymphocytes and susceptibility to HSV-1 corneal stromal disease. *Curr. Eye Res.* 10(Suppl): 47–53.
16. Stuart, P. M., B. Summers, J. E. Morris, L. A. Morrison, and D. A. Leib. 2004. CD8(+) T cells control corneal disease following ocular infection with herpes simplex virus type 1. *J. Gen. Virol.* 85: 2055–2063.
17. Nakanishi, Y., B. Lu, C. Gerard, and A. Iwasaki. 2009. CD8(+) T lymphocyte mobilization to virus-infected tissue requires CD4(+) T-cell help. *Nature* 462: 510–513.
18. Rajasagi, N. K., S. H. Kassim, C. M. Kollias, X. Zhao, R. Chervenak, and S. R. Jennings. 2009. CD4+ T cells are required for the priming of CD8+ T cells following infection with herpes simplex virus type 1. *J. Virol.* 83: 5256–5268.
19. Ghiasi, H., S. Cai, G. C. Perng, A. B. Nesburn, and S. L. Wechsler. 2000. Both CD4+ and CD8+ T cells are involved in protection against HSV-1 induced corneal scarring. *Br. J. Ophthalmol.* 84: 408–412.
20. Mueller, S. N., W. Heath, J. D. McLain, F. R. Carbone, and C. M. Jones. 2002. Characterization of two TCR transgenic mouse lines specific for herpes simplex virus. *Immunol. Cell Biol.* 80: 156–163.
21. van Lint, A., M. Ayers, A. G. Brooks, R. M. Coles, W. R. Heath, and F. R. Carbone. 2004. Herpes simplex virus-specific CD8+ T cells can clear established lytic infections from skin and nerves and can partially limit the early spread of virus after cutaneous inoculation. *J. Immunol.* 172: 392–397.
22. Wareing, M. D., A. B. Lyon, B. Lu, C. Gerard, and S. R. Sarawar. 2004. Chemokine expression during the development and resolution of a pulmonary leukocyte response to influenza A virus infection in mice. *J. Leukoc. Biol.* 76: 886–895.
23. Conrady, C. D., H. Jones, M. Zheng, and D. J. J. Carr. 2011. A functional type I interferon pathway drives resistance to cornea herpes simplex virus type 1 infection by recruitment of leukocytes. *J Biomed Res* 25: 111–119.
24. Conrady, C. D., W. P. Halford, and D. J. Carr. 2011. Loss of the type I interferon pathway increases vulnerability of mice to genital herpes simplex virus 2 infection. *J. Virol.* 85: 1625–1633.
25. Wuest, T. R., and D. J. Carr. 2010. VEGF-A expression by HSV-1-infected cells drives corneal lymphangiogenesis. *J. Exp. Med.* 207: 101–115.
26. Wuest, T. R., and D. J. Carr. 2008. Dysregulation of CXCR3 signaling due to CXCL10 deficiency impairs the antiviral response to herpes simplex virus 1 infection. *J. Immunol.* 181: 7985–7993.
27. Christensen, J. E., C. de Lemos, T. Moos, J. P. Christensen, and A. R. Thomsen. 2006. CXCL10 is the key ligand for CXCR3 on CD8+ effector T cells involved in immune surveillance of the lymphocytic choriomeningitis virus-infected central nervous system. *J. Immunol.* 176: 4235–4243.
28. Thapa, M., R. S. Welner, R. Pelayo, and D. J. Carr. 2008. CXCL9 and CXCL10 expression are critical for control of genital herpes simplex virus type 2 infection through mobilization of HSV-specific CTL and NK cells to the nervous system. *J. Immunol.* 180: 1098–1106.
29. Wuest, T., M. Zheng, S. Efstathiou, W. P. Halford, and D. J. J. Carr. 2011. The herpes simplex virus-1 transactivator infected cell protein-4 drives VEGF-A dependent neovascularization. *PLoS Pathog.* 7: e1002278.
30. Olsson, A. K., A. Dimberg, J. Kreuger, and L. Claesson-Welsh. 2006. VEGF receptor signalling - in control of vascular function. *Nat. Rev. Mol. Cell Biol.* 7: 359–371.
31. Mor, F., F. J. Quintana, and I. R. Cohen. 2004. Angiogenesis-inflammation cross-talk: vascular endothelial growth factor is secreted by activated T cells and induces Th1 polarization. *J. Immunol.* 172: 4618–4623.
32. Maertzdorf, J., G. M. Verjans, L. Remeijer, A. van der Kooi, and A. D. Osterhaus. 2003. Restricted T cell receptor beta-chain variable region protein use by cornea-derived CD4+ and CD8+ herpes simplex virus-specific T cells in patients with herpetic stromal keratitis. *J. Infect. Dis.* 187: 550–558.
33. Lepisto, A. J., G. M. Frank, M. Xu, P. M. Stuart, and R. L. Hendricks. 2006. CD8 T cells mediate transient herpes stromal keratitis in CD4-deficient mice. *Invest. Ophthalmol. Vis. Sci.* 47: 3400–3409.
34. Divito, S. J., and R. L. Hendricks. 2008. Activated inflammatory infiltrate in HSV-1-infected corneas without herpes stromal keratitis. *Invest. Ophthalmol. Vis. Sci.* 49: 1488–1495.
35. Xu, M., A. J. Lepisto, and R. L. Hendricks. 2004. CD154 signaling regulates the Th1 response to herpes simplex virus-1 and inflammation in infected corneas. *J. Immunol.* 173: 1232–1239.
36. Ambati, B. K., M. Nozaki, N. Singh, A. Takeda, P. D. Jani, T. Suthar, R. J. Albuquerque, E. Richter, E. Sakurai, M. T. Newcomb, et al. 2006. Corneal avascularity is due to soluble VEGF receptor-1. *Nature* 443: 993–997.
37. Lim, L., K. Pesudovs, and D. J. Coster. 2000. Penetrating keratoplasty for keratoconus: visual outcome and success. *Ophthalmology* 107: 1125–1131.
38. Epstein, R. J., J. A. Seedor, N. G. Dreizen, R. D. Stulting, G. O. Waring, III, L. A. Wilson, and H. D. Cavanagh. 1987. Penetrating keratoplasty for herpes simplex keratitis and keratoconus. Allograft rejection and survival. *Ophthalmology* 94: 935–944.
39. Pavan-Langston, D., and M. B. Abelson. 1978. Glucocorticoid therapy in ocular herpes simplex. II. Advantages. *Surv. Ophthalmol.* 23: 35, 43–47.
40. Saravia, M., G. Zapata, P. Ferraiolo, L. Racca, and A. Berra. 2009. Anti-VEGF monoclonal antibody-induced regression of corneal neovascularization and inflammation in a rabbit model of herpetic stromal keratitis. *Graefes Arch. Clin. Exp. Ophthalmol.* 247: 1409–1416.
41. de Nadaï, P., C. Chenivesse, J. Gilet, H. Porte, H. Vorng, Y. Chang, A. F. Walls, B. Wallaert, A. B. Tonnel, A. Tsicopoulos, and H. G. Zerwes. 2006. CCR5 usage by CCL5 induces a selective leukocyte recruitment in human skin xenografts in vivo. *J. Invest. Dermatol.* 126: 2057–2064.
42. Dufour, J. H., M. Dziejman, M. T. Liu, J. H. Leung, T. E. Lane, and A. D. Luster. 2002. IFN-gamma-inducible protein 10 (IP-10; CXCL10)-deficient mice reveal a role for IP-10 in effector T cell generation and trafficking. *J. Immunol.* 168: 3195–3204.
43. Wendel, M., I. E. Galani, E. Suri-Payer, and A. Cerwenka. 2008. Natural killer cell accumulation in tumors is dependent on IFN-gamma and CXCR3 ligands. *Cancer Res.* 68: 8437–8445.
44. Zhang, B., Y. K. Chan, B. Lu, M. S. Diamond, and R. S. Klein. 2008. CXCR3 mediates region-specific antiviral T cell trafficking within the central nervous system during West Nile virus encephalitis. *J. Immunol.* 180: 2641–2649.
45. Thapa, M., and D. J. Carr. 2009. CXCR3 deficiency increases susceptibility to genital herpes simplex virus type 2 infection: Uncoupling of CD8+ T-cell effector function but not migration. *J. Virol.* 83: 9486–9501.
46. Carr, D. J., T. Wuest, and J. Ash. 2008. An increase in herpes simplex virus type 1 in the anterior segment of the eye is linked to a deficiency in NK cell infiltration in mice deficient in CXCR3. *J. Interferon Cytokine Res.* 28: 245–251.
47. Lundberg, P., H. Openshaw, M. Wang, H. J. Yang, and E. Cantin. 2007. Effects of CXCR3 signaling on development of fatal encephalitis and corneal and periocular skin disease in HSV-infected mice are mouse-strain dependent. *Invest. Ophthalmol. Vis. Sci.* 48: 4162–4170.